Electronic supplementary material (ESM)

ESM Methods

Animal care and generation of mice

We obtained *Mc4r*$^{loxP/loxP}$ mice[1] from Dr. David P. Olson (University of Michigan) with permission from Dr. Bradford B. Lowell (Harvard University). We crossed these mice with *Sim1*^{cre} (006395, the Jackson Lab, USA) to knockout *Mc4r* predominantly in the PVH[1] (including some other regions that express *Sim1* gene). Some cohorts of MC4R-deficient mice were fed 75–80% of the average daily food consumed by their WT littermates immediately after weaning to prevent the development of obesity and match their body weights with that of their lean littermate controls as described previously[2, 3]. Dr. Steven Ebert provided adrenaline-deficient mice (phenylethanolamine N-methyltransferase, *Pnmt,* knockout) that were generated by his team as described previously[4]. All the mouse strains used in this study were backcrossed at least 6 times on C57BL/6 genetic background. Moreover, we used aspen wood shavings for bedding in the mouse cages to minimize the possibility of mice consuming the bedding during their fasting period as recommended by the Jackson Lab[5] and supported by our previous studies[2, 3].

Restoration of *Mc4r* in different brain regions

Mc4r$^{loxTB/loxTB}$ mice were anesthetized with isoflurane, placed in a stereotaxic frame (Model 1900, Kopf Instruments, USA) and the skull was exposed for intracranial injections of AAV-Cre or AAV-GFP (50nl, serotype 2, titer 8×10^{12} vg/ml, bilateral) using the following coordinates with reference to Bregma, PVH: anteroposterior (AP),

−0.70mm, mediolateral (ML), ±0.22mm, dorsoventral (DV), −4.80 mm; medial amygdala: AP, −1.5 mm, ML, ±2 mm, DV: −5.0 mm; lateral hypothalamus: AP, −1.5 mm; ML, ±1 mm, DV −5.1 mm; RVLM: from lambda, AP, -1.8, ML, ±1.2, DV –5.5 mm; NTS: head down at 45^0, reference: calamus scriptorius, AP, 0.35 mm; ML ± 0.15 mm; DV, -0.3 mm). We confirmed the accuracy of the injections by measuring *Mc4r* expression in each of the above-mentioned regions using qPCR at the end of the study. For qPCR, mouse brain was flash frozen and sliced using a cryostat up to the above-mentioned distances from bregma for each region and different areas were punched out bilaterally using a blunt 18G needle.

qPCR

Total RNA was extracted using E.Z.N.A total RNA kit II (Omega, USA) and reverse transcription to generate cDNA was performed with 500 ng total RNA and random hexamer primers (iScript cDNA synthesis kit, Bio-Rad, USA). qPCR was performed using a StepOne Real Time PCR System (Applied Biosystems, USA) and SYBR Green Master Mix (Bio-Rad, USA). We used the following primers, *Mc4r*: 5'-GCT GTC CGA GTA AAT GAT GAA GA-3'and 5' CGC TCC AGT ACC ATA ACA TCA-3'; *Pnmt*: 5'-CCG GAG CCA ATA TCA ATG AGA-3' and 5-'GAC CTG AGC AAC CCT GAT G-3'. All primers were used at a final concentration of 500 nM. The relative quantity of each mRNA was calculated from standard curves comprising 1000-fold change, normalized to an internal control *Hprt,* and then normalized to the mean of corresponding controls.

Renal and adrenal sympathetic nerve activity

Sympathetic nerve activity was assessed using direct multifiber recording. Mice were anesthetized with an intraperitoneal injection of a ketamine (91 mg/kg)/xylazine (9.1 mg/kg) cocktail. Each mouse was intubated using polyethylene tubing (PE-50) to allow spontaneous breathing of oxygen enriched air throughout the experimental procedure. Next, a tapered micro-renathane tubing (MRE-040; Braintree Scientific, USA) was inserted into the right jugular vein from which α-chloralose was infused at an initial dose of 12 mg/kg during the surgical preparation then at a sustaining dose of 6 mg/kg/h; until completion of the study. Another tapered MRE-040 tubing was inserted into the left carotid artery for continuous measurement of arterial pressure. The carotid cannula was connected to a low-volume pressure transducer (BP-100; iWorks System, Inc., Dover, NH) that led to an ETH-250 Bridge/Bio Amplifier (CB Sciences, USA). The filtered, amplified pulsatile pressure signal was directed to an analog digital acquisition system (MacLab 8S) for continuous display of phasic arterial pressure and heart rate on a computer monitor. Core body temperature of the mouse was measured and maintained at a constant temperature of 37.5˚C using a temperature controller (Physitemp, Model TCAT-2; Braintree Scientific, USA).

The mouse was positioned on its right side to access the renal and then adrenal sympathetic nerves. As described previously[6], post-ganglionic fibers innervating the left kidney were first identified, dissected free, and placed on a bipolar 36-gauge platinum-iridium electrode (A-M Systems, Carlsborg, USA). Kwik-Sil (WPI, USA) was applied to protect and to maintain the renal nerve/electrode connection throughout the protocol. The recording electrode was connected to a high impedance probe (HIP-511;

Grass Instruments, USA), and the nerve signal was amplified 10^5 times with a Grass P5 AC pre-amplifier and filtered at low and high frequency cutoffs of 100 Hz and 1000 Hz, respectively. This nerve signal was directed to a speaker system and to an oscilloscope (54501A, Hewlett-Packard, USA) for auditory and visual monitoring of the nerve activity. The signal was then directed to a resetting voltage integrator (B600C, University of Iowa Bioengineering) that sums the total voltage output in units of 1 V *sec before resetting to zero and counting the number of spikes per second. The final neurograms were continuously routed to a MacLab analogue-digital converter (8S, AD Instruments Castle Hill, New South Wales, Australia) for permanent recording and data analysis on a Macintosh computer. Basal arterial pressure, heart rate and renal sympathetic nerve activity were recorded and measured continuously for 30 minutes after a stable state of anesthetic level and constant body temperature of 37.5˚C were achieved. At the end of 30 min, the renal nerve was sectioned to account for any background noise in the assessment of sympathetic outflow in the integrated voltage and spike frequency.

In the same mouse, pre-ganglionic nerve serving the left adrenal gland was next identified, dissected free, and placed on the same bipolar 36-gauge platinum-iridium electrode. Adrenal sympathetic nerve activity was recorded in the same manner as described above for the renal nerve activity. Again, basal arterial pressure, heart rate and adrenal sympathetic nerve activity were recorded and measured continuously for 30 min after a stable state of anesthetic level and constant body temperature of 37.5˚C were achieved. At the end of 30 min, adrenal sympathetic nerve activity was corrected for post-mortem background activity to eliminate background electrical noise.

Graded [$^{13}C_6$] glucose infusion procedure

For graded glucose infusion, mice were anesthetized using isoflurane (3-5% for induction and 2-3% for maintenance) before making a midline laparotomy incision from the pelvis to the sternum. Then a cannula was inserted each into the jugular vein, carotid artery, and urinary bladder with a 2 cm PE 50 tubing to collect urine samples. Following a 60 min. equilibration period with baseline [$^{13}C_6$] glucose infusion (5 mM glucose in saline, 50 µl/h), we infused 5% [$^{13}C_6$] glucose solution at a rate of 20, 40, 60 and 80 µl/h for 30 min. each sequentially in the same mouse over 120 min. to increase blood [$^{13}C_6$] glucose levels during the experiment. This protocol provides blood glucose range of 5 to 28 mM based on pilot studies in our lab. Blood (20 µl) and urine (10 µl) samples were collected at 10 min. intervals to measure [$^{13}C_6$] glucose. The lost blood cells in the experimental mice were replenished by infusing saline-washed erythrocytes obtained from donor mice.

Western blotting

We performed western blot as per our published protocol[2]. Rabbit polyclonal anti-GLUT2 (600-401-GN3; Rockland Immunochemicals, USA), rabbit polyclonal anti-SGLT2 (ab37296, Abcam, USA), rabbit polyclonal anti-SGLT1 (ab14686, Abcam, USA), rabbit polyclonal anti-GLUT1 (ab652, Abcam,USA), and rabbit polyclonal anti- Na^+/K^+-ATPase (3010, Cell signaling Technology, USA) primary antibodies were used at 1:1,000 dilutions, in tris-buffered saline with Tween 20 containing 5% powdered milk. Secondary antibody anti-rabbit (611-103-122; Rockland Immunochemicals, USA) coupled to horseradish peroxidase was used to detect the corresponding primary antibodies bound to their respective target proteins. We used vinculin (sc-73614; Santa

Cruz Biotechnology, USA) to confirm equal loading of samples and for normalizing the intensity of bands for glucose transporters and Na^+/K^+-ATPase. When feasible, we cut the blots horizontally just above ~80KDa to examine the internal control at the same time as the proteins of interest on the same membrane. Alternatively, we stripped the blots to remove primary and secondary antibodies after imaging proteins of interest and used the same blots for probing the internal control. Luminescence was generated with ECL substrate (34095; Thermo Scientific, USA) and recorded on a BioRad imaging System. All the antibodies were tested for specificity using their corresponding positive controls (lysate from cells overexpressing the protein of interest, ESM Fig. 6f, g).

ESM Table 1. Urine glucose parameters in 24-wk-old C57Bl/6 mice.

	Urine glucose concentration (mmol/l)		Urine volume (ml)		Urine glucose amount (µg/24h)	
MALE	**WT**	***Mc4r*$^{-/-}$**	**WT**	***Mc4r*$^{-/-}$**	**WT**	***Mc4r*$^{-/-}$**
Baseline, n=7	0.25 ±0.03	0.85 ±0.1 ***	0.76 ±0.2	2.21 ±0.3 **	30 ±5	350 ±76 **
Oral glucose challenge, n=5 or 6	0.96 ±0.2	5.4 ±0.6 ***	0.69 ±0.1	3.8 ±0.5 ***	110 ±21	3,470 ±345 ***
Intraperitoneal glucose challenge, n=4 or 5	6.7 ±0.15	113 ±6.2 ***	0.8 ±0.1	2.2 ±0.4 *	965 ±127	44,749 ±8,746**
FEMALE						
Baseline, n=6 or 7	0.45 ±0.04	0.9 ±0.2 *	0.8 ±0.3	2.2 ±0.3 *	80 ±23	360 ±78 **
Oral glucose challenge, n=4 or 5	3.52 ±0.8	7 ±0.7 *	1 ±0.1	3.9 ±0.1 ***	614 ±126	4,850 ±486 ***
Intraperitoneal glucose challenge, n=4 or 6	10 ±0.2	118 ±5 ***	0.9 ±0.1	2.3 ±0.1 ***	1,609 ±243	48,453 ±3,370***

Results are presented as mean ±SEM of raw data. *p<0.05, **p<0.01, ***p<0.001. Two-tailed Student's t-test. Oral glucose administration was 250mg and intraperitoneal was 200mg glucose, Mc4r$^{-/-}$, *Mc4r*$^{loxtb/loxtb}$.

ESM Figures

ESM Fig. 1.

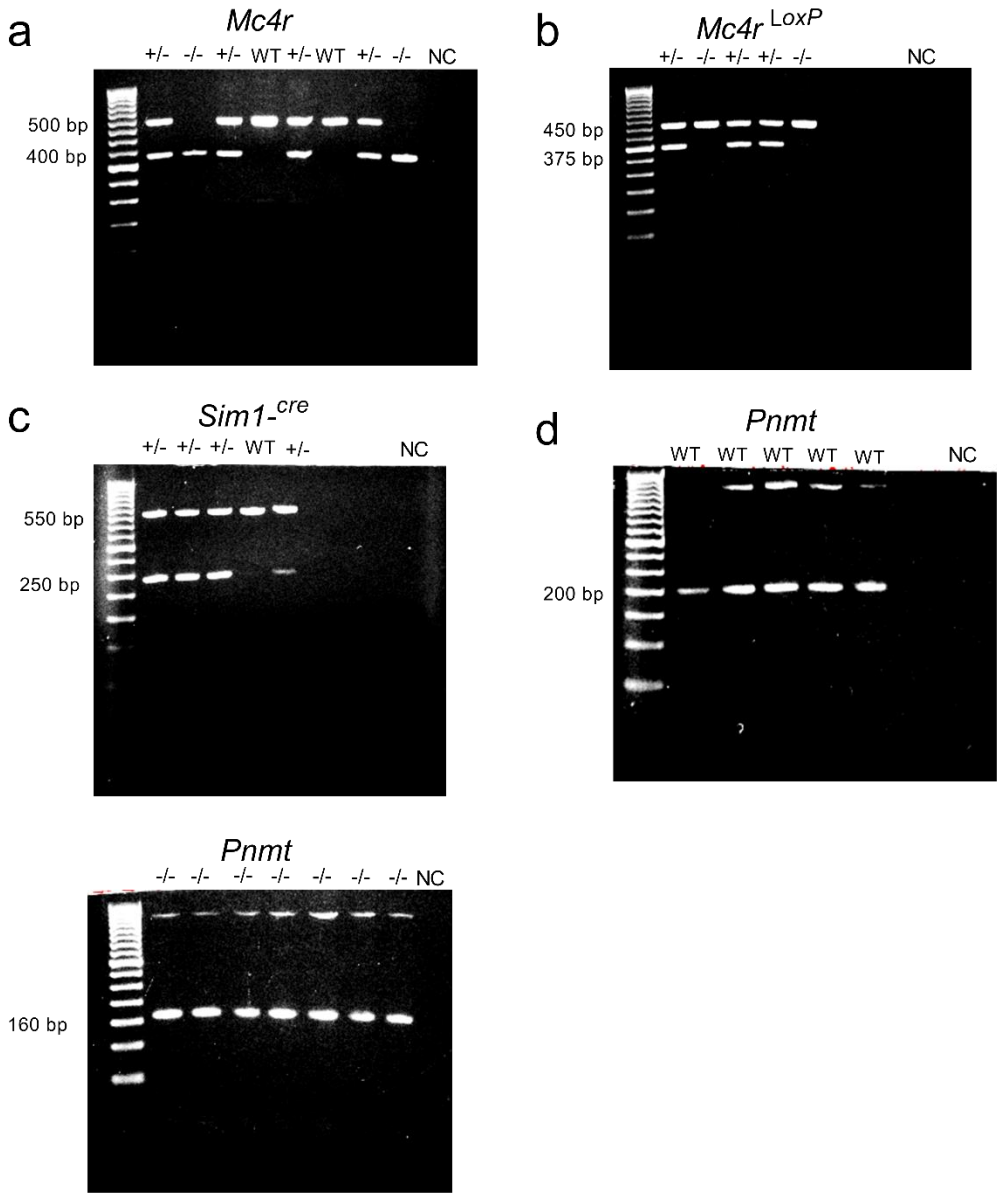

Representative genotypes of mice used in this study. **(a)** *Mc4r* null mouse model: *Mc4r* heterozygous *(Mc4r*$^{+/-}$; 500 and 400 bp), *Mc4r* homozygous *(Mc4r*$^{-/-}$; 400 bp), WT (500 bp); **(b)** *Mc4r*^{loxP} mouse model: *Mc4r*^{loxP} heterozygous *(Mc4r*$^{loxP/+}$; 450 and 375 bp), *Mc4r*^{loxP} homozygous *(Mc4r*$^{loxP/loxP}$; 450 bp); **(c)** Sim1^{cre} mouse model: Sim1^{cre} heterozygous (Sim1$^{cre\ +/-}$; 550 bp and 250 bp mark), WT (550 bp); **(d)** *Pnmt* KO mouse model: WT (200 bp); *Pnmt*$^{+/-}$ (200 and 160 bp); *Pnmt*$^{-/-}$ (160 bp). WT, wild type. NC, negative control.

ESM Fig. 2

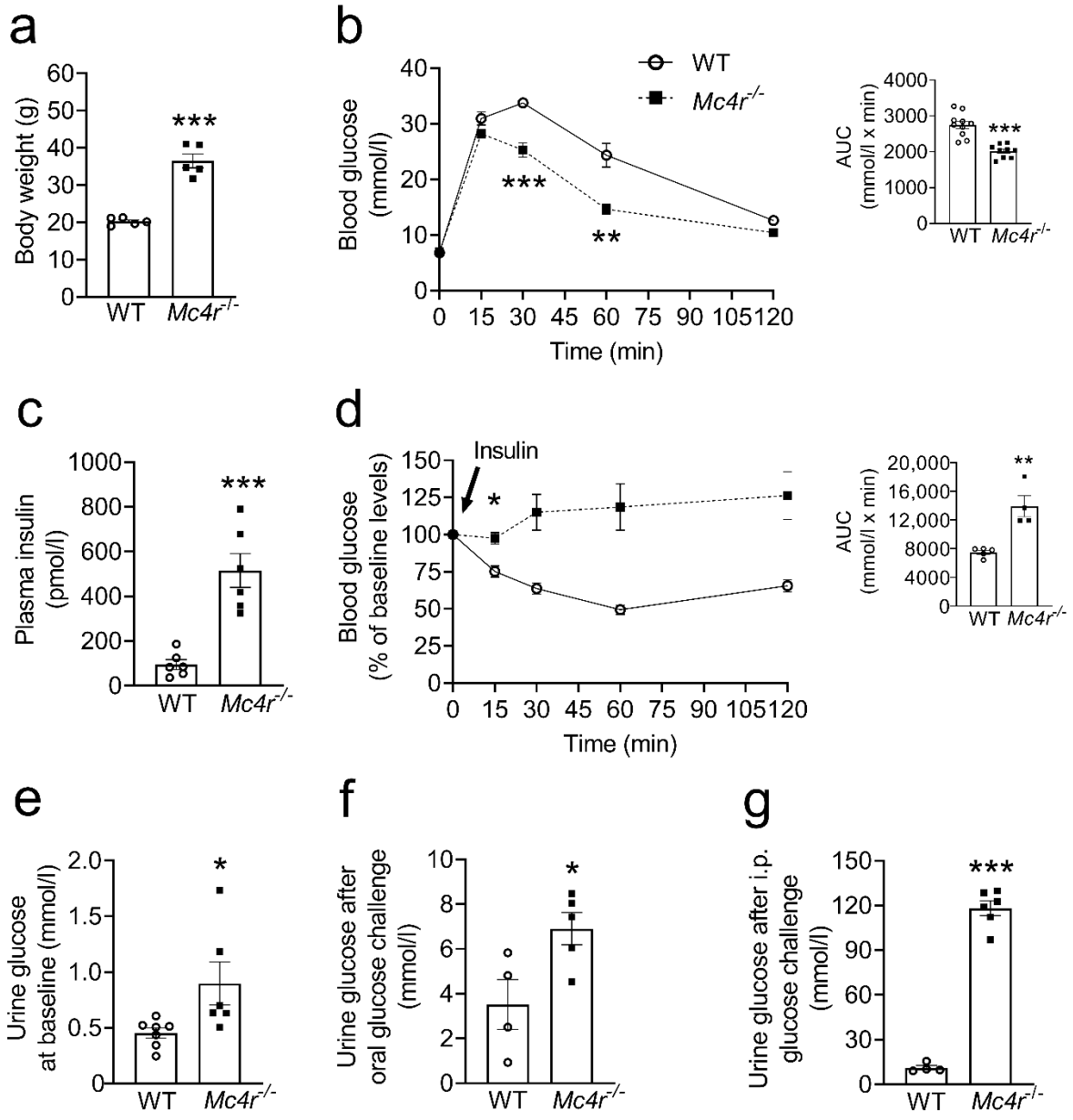

Improved glucose tolerance despite obesity and insulin resistance, and elevated glycosuria in 24-wk-old female *Mc4r* null C57Bl/6 mice. **(a)** Body weight; **(b)** Oral glucose tolerance test (OGTT), mice were fasted for 6h; **(c)** Fasting plasma insulin levels; **(d)** Insulin tolerance test (ITT); **(e)** 24h urine glucose concentration at baseline; **(f)** 24h urine glucose concentration after administering 250 mg of oral glucose in female *Mc4r* null mice; **(g)** 24h urine glucose concentration after administering 200 mg of ip glucose in female *Mc4r* null mice. Bar graphs in **(b)** and **(d)** represent the corresponding area under the curve. Two-tailed Student's t-test or repeated measures two-way ANOVA followed by Bonferroni's multiple comparison test were used for comparisons. *p<0.05, **p<0.01, ***p<0.001. n=4-10. Error bars are mean ± SEM. WT, wild type. *Mc4r*$^{-/-}$, *Mc4r*$^{loxtb/loxtb}$

ESM Fig. 3

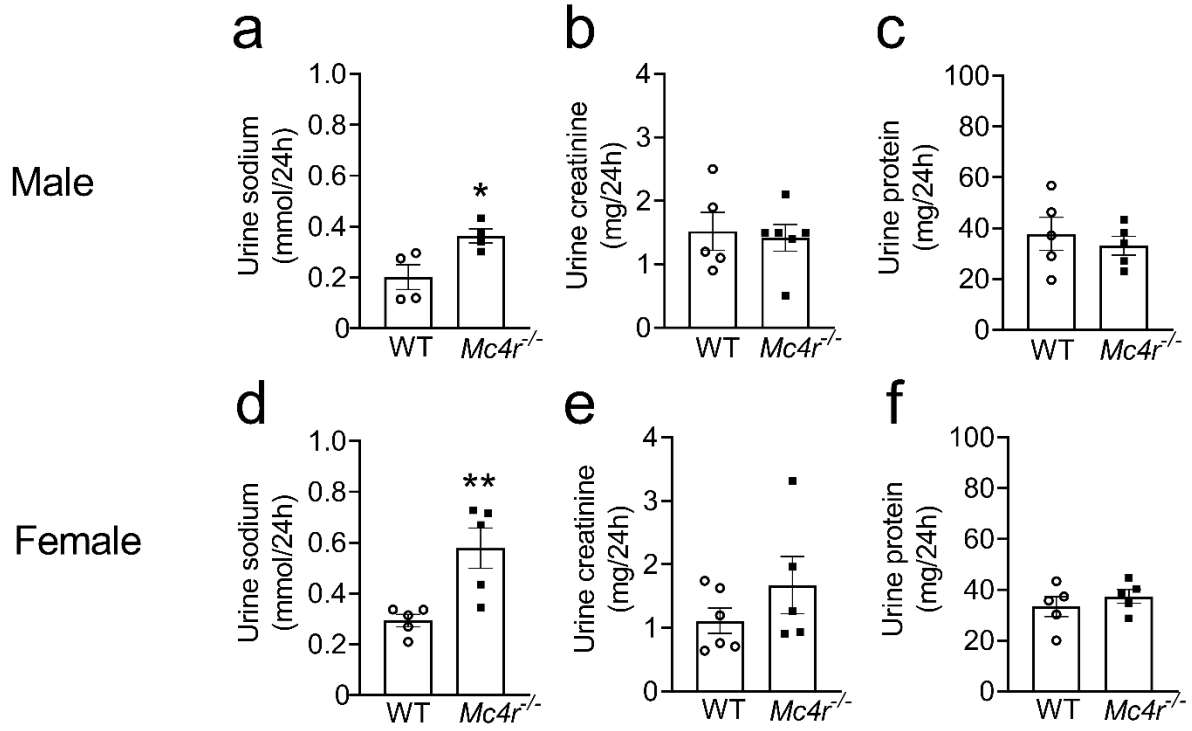

Urine electrolytes and total protein in 24-wk-old *Mc4r* null C57Bl/6 mice. **(a)** Urine sodium; **(b)** Urine creatinine; **(c)** Urine protein in 24-wk-old male *Mc4r* null C57Bl/6 mice; **(d)** Urine sodium; **(e)** Urine creatinine; **(f)** Urine protein in 24-wk-old female *Mc4r* null C57Bl/6 mice. Two-tailed Student's t-test was used for comparisons. *p<0.05, **p<0.01, n=4-6. Error bars are mean ± SEM. WT, wild type. *Mc4r*$^{-/-}$, *Mc4r*$^{loxtb/loxtb}$

ESM Fig. 4

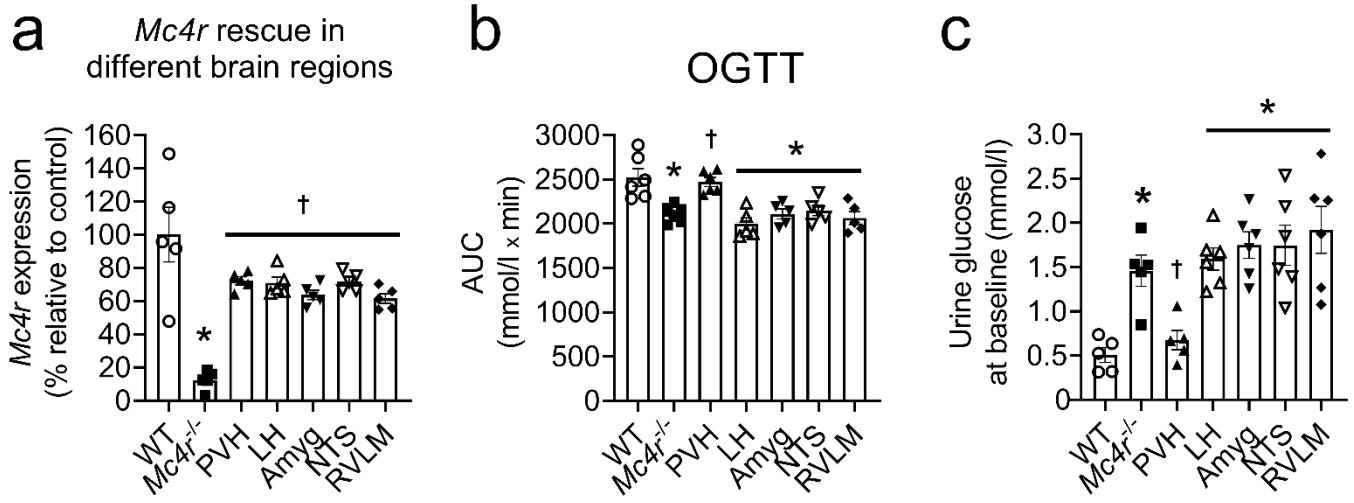

Rescue of *Mc4r* in the paraventricular nucleus of the hypothalamus (PVH) reversed the phenotype of improved glucose tolerance and elevated glycosuria in 16- to 24-wk-old reversible *Mc4r* null C57Bl/6 mice. **(a)** *Mc4r* expression after its rescue in different brain regions; **(b)** Oral glucose tolerance test (AUC; OGTT) after the *Mc4r* rescue, mice were fasted for 6h; **(c)** 24h urine glucose concentration at baseline after the *Mc4r* rescue in otherwise *Mc4r* null mice. Two-way ANOVA followed by Bonferroni's multiple comparison test was used for comparisons. *p<0.05 compared to WT; †p<0.05 compared to $Mc4r^{-/-}$. n=4-6. Error bars are mean ± SEM. WT, wild type. $Mc4r^{-/-}$, $Mc4r^{loxtb/loxtb}$. PVH, paraventricular nucleus of the hypothalamus; LH, lateral hypothalamus; Amyg, medial amygdala; NTS, nucleus tractus solitarius; RVLM, rostral ventrolateral medulla.

ESM Fig. 5

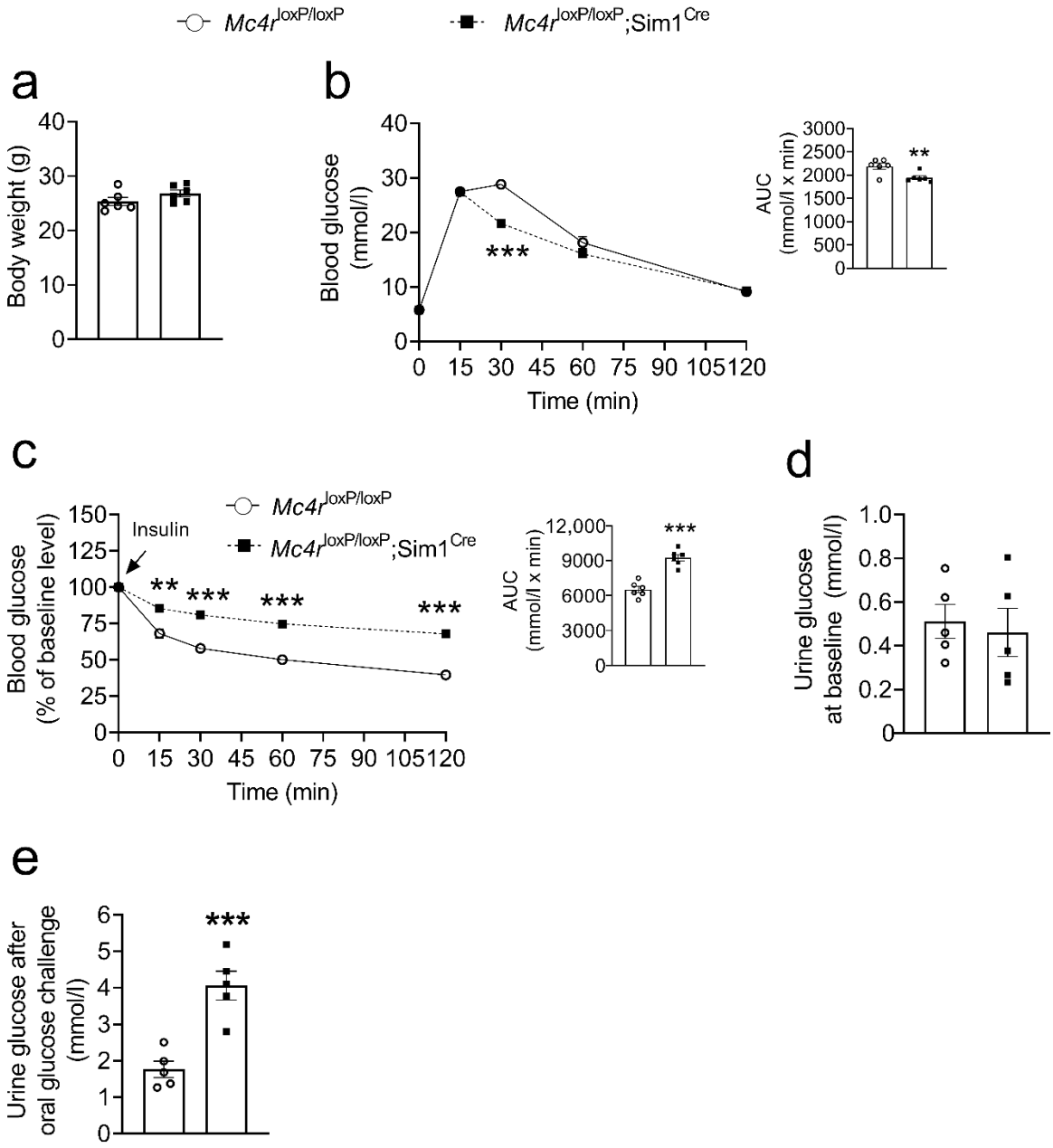

Improved glucose tolerance in the presence of insulin resistance in weight-matched 18- to 24-wk-old *Mc4r*$^{loxP/loxP}$;*Sim1*^{Cre} mice. **(a)** Body weight; **(b)** Oral glucose tolerance test (OGTT), mice were fasted for 6h; **(c)** Insulin tolerance test (ITT); **(d)** 24h urine glucose concentration at baseline; **(e)** 24h urine glucose concentration after administering 250 mg of oral glucose in *Mc4r*$^{loxP/loxP}$;*Sim1*^{Cre} mice. Bar graphs in **(b)** and **(c)** represent the corresponding area under the curve. Two-tailed Student's t-test or repeated measures two-way ANOVA followed by Bonferroni's multiple comparison test were used for comparisons. **p<0.01, ***p<0.001. n=5-6. Error bars are mean ± SEM.

ESM Fig. 6

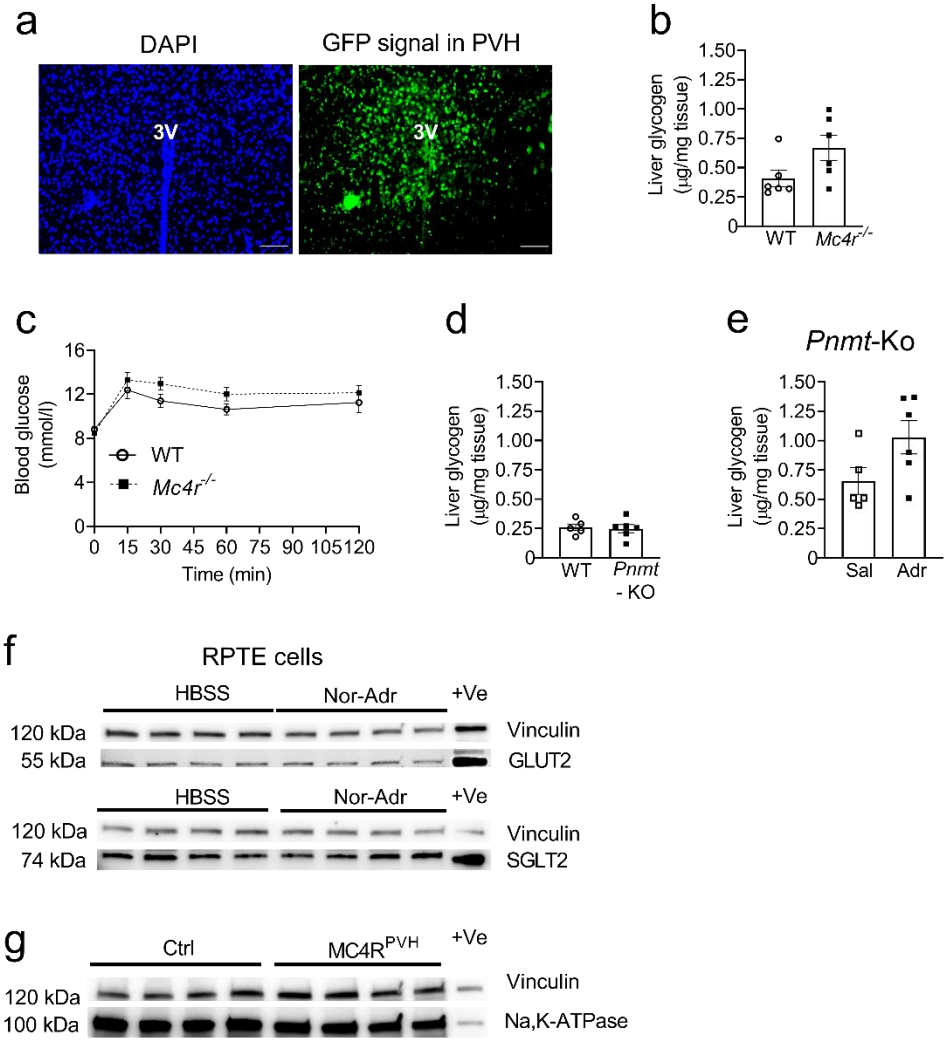

No change in glycogen levels and gluconeogenesis in obese male 24-wk-old *Mc4r* null and 6- to 9-wk-old adrenaline-deficient C57Bl/6 mice. **(a)** Representative image of GFP signal (fluorescence in situ hybridization) in the paraventricular nucleus of the hypothalamus (PVH), validating the accuracy of AAV-Cre-GFP injections in $Mc4r^{loxP/loxP}$ mice, scale bar 100µm; **(b)** Liver glycogen levels in overnight fasted mice; **(c)** Pyruvate tolerance test (PTT) in 6h fasted *Mc4r* null C57Bl/6 mice; **(d)** Liver glycogen levels in overnight fasted *Pnmt*-KO mice; **(e)** Liver glycogen levels in overnight fasted *Pnmt*-KO mice whose plasma adrenaline is restored; **(f)** GLUT2 and SGLT2 levels, with their positive controls to validate their antibodies, in mouse primary renal tubular (RPTE) cells treated with noradrenaline; **(g)** Positive control to validate Na^+/K^+-ATPase antibody. Proteins of interest and internal control were probed on the same membrane as described in Methods. Two-tailed Student's t-test or repeated measures two-way ANOVA followed by Bonferroni's multiple comparison test were used for comparisons. n=5-7. Error bars are mean ± SEM. WT, wild type. $Mc4r^{-/-}$, $Mc4r^{loxtb/loxtb}$. *Pnmt*-KO, phenylethanolamine N-methyltransferase knockout mice (adrenaline-deficient mice). Sal, Saline; Adr, Adrenaline; HBSS, Hanks' Balanced Salt Solution; Nor-Adr, Noradrenaline; +Ve, positive control.

ESM Fig. 7

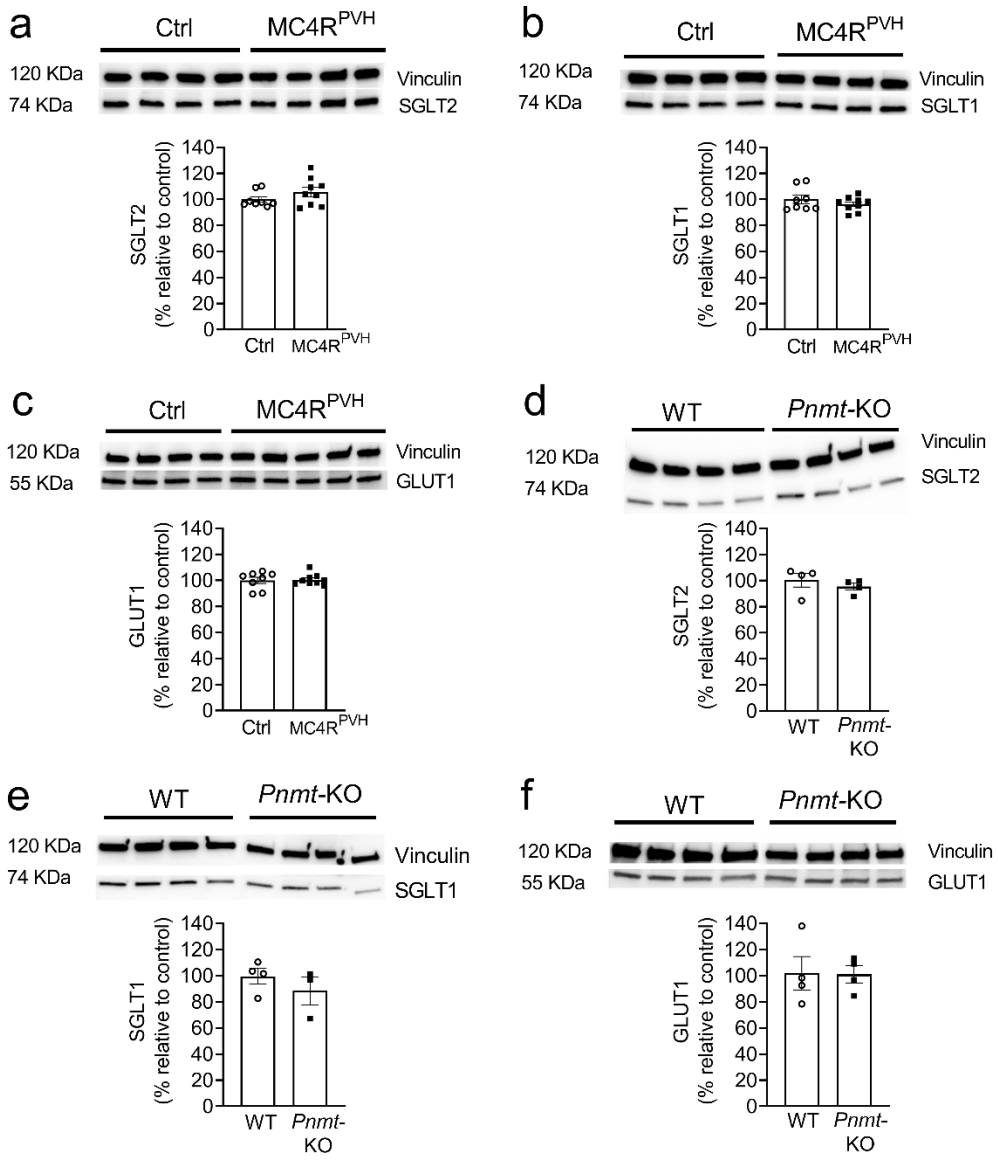

Representative western blots showing renal cortical glucose transporters in obese male *Mc4r*^{PVH}-deficient and adrenaline-deficient mice. Renal cortical **(a)** SGLT2; **(b)** SGLT1; **(c)** GLUT1 levels in *Mc4r*^{PVH}-deficient mice; Renal cortical **(d)** SGLT2; **(e)** SGLT1; **(f)** GLUT1 levels in adrenaline-deficient mice. Proteins of interest and internal control were probed on the same membrane as described in Methods. Two-tailed Student's t-test was used for comparisons. N=4-9. Error bars are mean ± SEM. WT, wild type; *Pnmt*-KO, phenylethanolamine N-methyltransferase knockout (adrenaline-deficient mice); SGLT2, Sodium–*glucose* cotransporter 2; SGLT1, Sodium–*glucose* cotransporter 1; GLUT1, Glucose transporter 1; Ctrl, *Mc4r*$^{loxP/loxP}$ with AAV-GFP; MC4R^{PVH}, *Mc4r*$^{loxP/loxP}$ with AAV-Cre.

ESM References

[1] Shah BP, Vong L, Olson DP, et al. (2014) MC4R-expressing glutamatergic neurons in the paraventricular hypothalamus regulate feeding and are synaptically connected to the parabrachial nucleus. Proceedings of the National Academy of Sciences 111(36): 13193. 10.1073/pnas.1407843111

[2] Chhabra KH, Adams JM, Fagel B, et al. (2016) Hypothalamic POMC Deficiency Improves Glucose Tolerance Despite Insulin Resistance by Increasing Glycosuria. Diabetes 65(3): 660-672. 10.2337/db15-0804

[3] Chhabra KH, Adams JM, Jones GL, et al. (2016) Reprogramming the body weight set point by a reciprocal interaction of hypothalamic leptin sensitivity and Pomc gene expression reverts extreme obesity. Mol Metab 5(10): 869-881. 10.1016/j.molmet.2016.07.012

[4] Ebert SN, Rong Q, Boe S, Pfeifer K (2008) Catecholamine-synthesizing cells in the embryonic mouse heart. Annals of the New York Academy of Sciences 1148: 317-324. 10.1196/annals.1410.008

[5] Garcia-Arocena D (2014) 7 TIPS EVERY DIO MICE USER SHOULD KNOW. In: https://wwwjaxorg/news-and-insights/jax-blog/2014/may/seven-tips-every-dio-mice-user-should-know; date of access: 05/11/2019

[6] Bell BB, Harlan SM, Morgan DA, Guo DF, Cui H, Rahmouni K (2018) Differential contribution of POMC and AgRP neurons to the regulation of regional autonomic nerve activity by leptin. Mol Metab 8: 1-12. 10.1016/j.molmet.2017.12.006